Deformation Band Studies of Axially Compressed Poly(*p*-Phenylene Terephthalamide) Fiber

T. TAKAHASHI, M. MIURA, and K. SAKURAI, *Faculty of Engineering, Fukui University, Bunkyo 3-9-1, Fukui 910, Japan*

Synopsis

Deformation mechanism of poly(*p*-phenylene terephthalamide) (PPTA) fiber during axial compression was studied. PPTA fibers were embedded in resin and axialy compressed in a tensile machine. PPTA fibers were then taken out from resin at various stages of compression. Kink band formation was examined by means of polarizing microscopy, X-ray diffraction (WAXD), electron diffraction (ED), and electron microscopy. WAXD pattern of seriously compressed PPTA fiber shows that (200) reflection spots and arcs appear on the equator and meridian respectively. On the other hand, (110) reflection spots are confined to the equator. PPTA fiber could be splitted tangentially and radially into two kinds of thin fibrillar fragments (I and II) which reveal two distinct types of kink band and ED pattern. In fragment I obtained by tangential splitting, kink bands are formed at about 55° with respect to fibril axis, whereas in fragment II obtained by radial splitting kink bands are formed perpendicular to the fibril axis. These results were confirmed by ED studies. It was assumed that slip of (200) planes containing hydrogen bonded sheets as well as intermicrofibril slip plays an important role in the deformation of PPTA fiber during axial compression.

INTRODUCTION

Mechanical properties and supermolecular structures of high modulus poly(*p*-phenylene terephthalamide) (PTTA) fiber have been investigated by many workers. Dobb et al. proposed a radially arranged pleated sheet organization for PPTA fiber.[1] It would be predicted that the supermolecular structure would lead to a low compressive strength of the fiber.

The present work is concerned with kink band formation of PPTA fiber during axial compression. It is well known that the kink bands are formed when oriented specimens of flexible polymers, such as polyethylene, polypropylene, nylon, poly(ethylene terephthalate, are axially compressed,[2,3] twisted,[4,5] or redrawn[6–9] at various angles to the original direction. It is interesting to investigate the structures of axially compressed PPTA fiber comparing with those of the deformed flexible polymers.

A crystallographic explanation of the kink band formation has been given in terms of electron diffraction (ED) pattern, bright-field (BF) image, and dark-field (DF) images formed from (*hk*0) and (00*l*) reflections. It was confirmed that slip of crystallographic planes containing hydrogen-bonded sheets as well as intermicrofibril slip plays an important role in the deformation of PPTA fiber during the axial compression.

EXPERIMENTAL

Commercially available PPTA fiber (Kevlar 29: $[\eta] = 4.5$) was used. PPTA fibers were embedded in 2-hydroxypropyl methacrylate. A cylindrical resin

Journal of Applied Polymer Science, Vol. 28, 579–586 (1983)
 CCC 0021-8995/83/020579-08$01.80

block, 7 mm in length and 7.5 mm in diameter, containing PPTA fibers was axially compressed in a tensile machine (Shimadzu Autograph IS-2000) with a speed of 1.5 mm/min.

Deformed PPTA fibers were taken out from a resin block by treating with dimethyl sulfoxide. Wide-angle X-ray diffraction pattern was recorded in a flat-plate camera, utilizing nickel-filtered CuK_α radiation. For electron microscopic studies, compressed PPTA fiber was peeled into fibrillar fragments in water with the aid of needles, followed by mild sonication.[10] The fragments were deposited on carbon–collodion-coated grids. Specimens for BF image and ED studies were shadowed with gold–paradium alloy. ED pattern was produced from specimen area of 3 μm in diameter. A transmission electron microscope (Nihon-Denshi: JEOL 200B) and scanning electron microscope (Hitachi: HSM-2A) were used throughout this work.

RESULTS AND DISCUSSIONS

PPTA fibers embedded in resin were axially compressed in a tensile machine. Figure 1 shows an obtained stress–strain curve. Because of a low fiber density (about 0.2 wt %) in matrix resin, the stress–strain curve is dominated by the resin. When the resin block is compressed with a low speed (0.5 mm/min = 6.7%/min), true material yield with uniform deformation occurred at the yield point. Samples were taken out at various stages of compression. Five samples (original sample A, compressed samples B, C, D, and E) were obtained.

Optical Microscopic and SEM Observations

Original and axially compressed PPTA fibers were examined by means of polarizing optical microscope with the polars crossed. Optical micrographs of the samples A, C, D, and E at the diagonal position are shown in Figure 2(a). As the compression proceeds, dark lines appear at angles of 50–60° with respect to the fibril axis. Dark lines develop with increasing strain up to yield point, while the angles between dark lines and the fiber axis are almost independent of the strain. Konopasek and Hearle also observed the dark lines for PPTA fibers

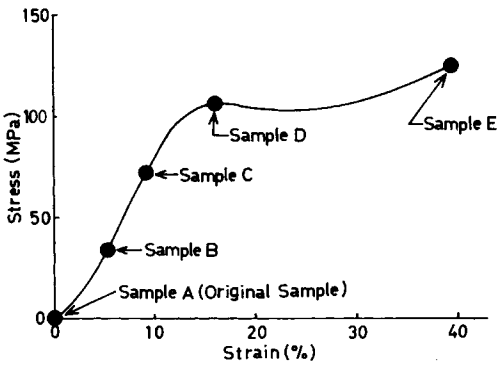

Fig. 1. Stress–strain curve for PPTA fiber/resin composite. A cyclindrical resin block containing PPTA fiber was axially compressed in a tensile machine. Sample A is original sample. Four samples, B, C, D, and E were taken out at various stages of compression.

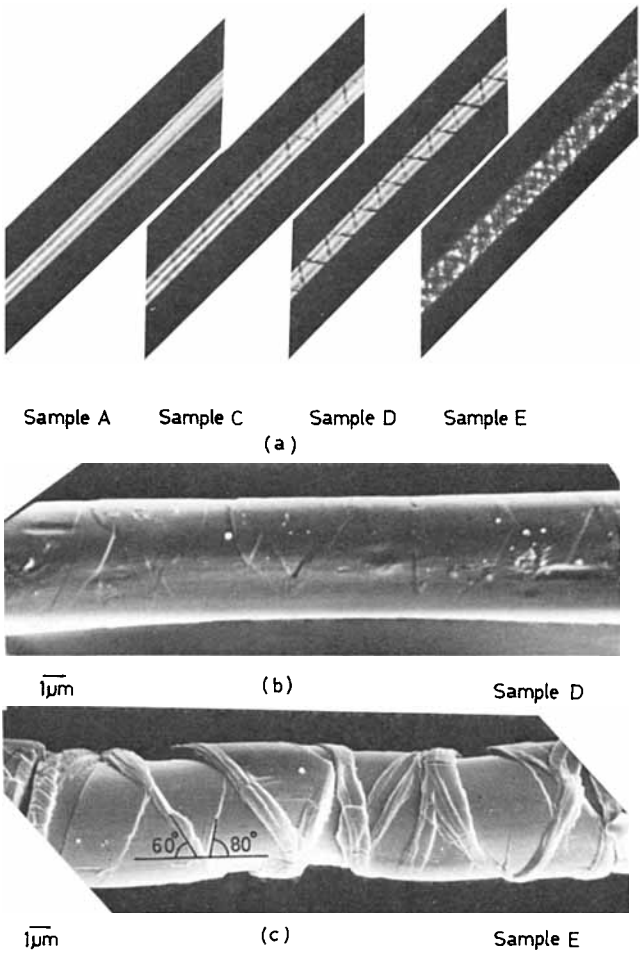

Fig. 2. (a) Polarizing optical micrographs of original sample (sample A) and samples C, D, and E. (b) SEM micrograph of sample D. (c) SEM micrograph of sample E.

which are subjected to tensile fatigue test.[11] It is obvious that the dark lines come from the kink band, where molecular chains are sharply bent.

It seems that samples C and D reveal "helix-like" lines. Sample B does also, though with a less intense development. It is difficult, however, to determine if the deformation is helix, because, as SEM photograph of sample D [Fig. 2(b)] shows, many deformation bands alternating in angle are observed on the surface of the sample.

Figures 1 and 2 indicate that the structure of PPTA fiber changes remarkably after a yield point of the stress–strain curve of the PPTA fiber–resin composite. In fact, sample E becomes thick by 44% in diameter corresponding to axial compression. Because of the voids, this sample already lost its transparency. As can be seen in optical and SEM photographs, sample E has very complicated appearance. SEM photograph of sample E [Fig. 2(c)] shows that kink bands are formed at angles of 60–80° to fiber axis. Kink band angles in sample E are fairly larger than those in sample D. These results suggest that the kink bands formed in the initial stage are further squashed after the yield point. Intersection

of the kink bands is also observed in the same photograph [Fig. 2(c)]. In addition to the generation of new kink bands, development and intersection of the kink band after the yield point may further complicate the appearance of sample E.

X-Ray Diffraction Studies

Wide-angle X-ray diffraction (WAXD) patterns of the original sample (sample A), and axially compressed PPTA fiber (samples C and E) are shown in Figure 3. All reflections can be interpreted on the basis of Northholt's monoclinic cell.[12] Amorphous halo at about $2\theta = 20°$ comes from remaining resin which was used for embedding. In WAXD patterns of samples A and C, (110) and (200) reflection spots are visible only on the equator. Sample C give a WAXD pattern similar to that of original sample, because the amount of crystals in the kink bands is still very small.

Figures 3(c) and (d) are a WAXD pattern and corresponding scheme for sample E. Interestingly, the (200) reflection appear not only on the equator as spots but also on the meridian as arcs. On the other hand, the (110) reflection spots are confined to the equator. It is confirmed, by quantitative azimuthal scanning, that (200) arcs on the meridian are resolved into two maximum located at azimuthal angles of ±12°. It is reasonable to assume that these two off-meridional

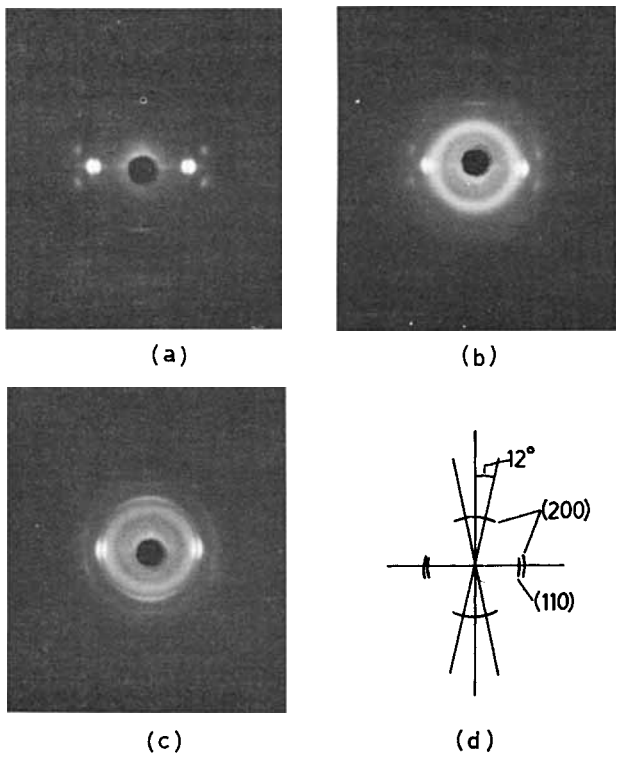

Fig. 3. Wide-angle X-ray diffraction (WAXD) patterns of original and axially compressed samples. (a) Original sample (sample A). (b) Sample C. (c) Sample E. (d) Scheme of WAXD pattern for sample E. Off-meridional (200) arcs are visible in WAXD pattern for sample E.

arcs originate from crystals inside the kink band and the azimuthal angle of (200) arcs corresponds to the inclination angle of the kink bands with respect to fiber axis. This result is consistent with SEM observation. The existence of the off-meridional (200) reflection suggests that local crystalline slip on (200) planes along the c-axis contributes to the formation of the kink band.

Electron Diffraction and Dark-Field Image Studies

Previous workers have proposed a radial and tangential morphology for PPTA fiber on the basis of electron microscopy of longitudinal and cross sections. Hagege et al. suggested that PPTA fiber tends to be splitted tangentially and radially.[13] In our case, PPTA fiber could also be splitted tangentially and radially into two kinds of thin fibrillar fragments which reveal two distinct types of kink band and ED pattern, respectively.

Figures 4(a) and (b) show an electron micrograph and corresponding ED pattern of fibrillar fragment. This ED pattern comes from the region of about 3-μm diameter. As Figure 4(a) shows, kink bands are formed at 55° with respect to the fibril axis. Arrows in the kink band indicate the direction of microfibrils. Microfibrils close to the kink boundary are almost at a right angle to the kink boundary, while microfibrils in the central region of the kink band are inclined by 20° to the original fibril axis. Figure 4(a) also shows that kink band formation is accompanied by fibrillation and intermicrofibril slip. It can be assumed that, in addition to the crystalline slip along the c-axis, intermicrofibril slip also enables the microfibrils to alternate their direction with respect to the fibril axis.

The fragment with this type of kink bands generally gives strong (200) reflections as shown in Figure 4, indicating the preferred orientation of the b-axis

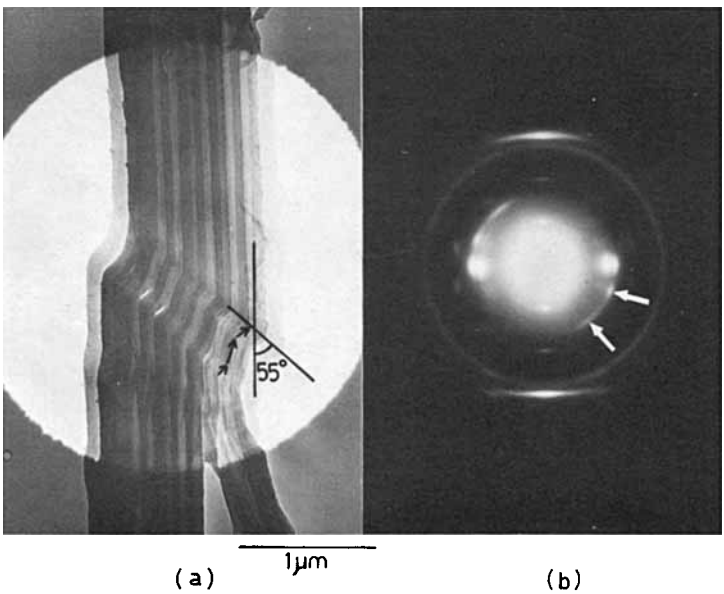

Fig. 4. Electron micrograph and corresponding electron diffraction pattern of a fibrillar fragment which was taken out from sample E by tangential splitting. Kink band is formed at 55° with respect to fibril axis.

perpendicular to the fragment surface. This means that the b-axis almost parallel to an electron beam. However, because of the fluctuation of the orientation of the b-axis, (110) reflection arcs are also visible. Considering the fact that hydrogen-bonded sheets of PPTA crystal orient perpendicular to the fragment surface, it is reasonable to conclude that the fragment shown in Figure 4(a) was taken out of PPTA fiber by tangential splitting. It is obvious that off-equatorial (200) reflection spots exactly correspond to the crystals in the kink band. On the other hand, (110) reflections are observed only on the equator. The ED pattern shown in Figure 4(b) indicates that the kink bands are formed by slip of (200) plane along the molecular axis.

The inclination angles of microfibrils inside the kink band are apparently in conflict with X-ray results. As the WAXD pattern of sample E [Fig. 3(c)] shows, the (200) reflection appears near the meridian. Serious compressed fiber (sample E) might be elongated during fragmentation as if smoothing out a crumpled paper.

Figures 5(a) and (b) show an electron micrograph of another type of fragment and corresponding ED pattern, respectively. Figure 5(a) indicates that kink bands are formed perpendicular to the fibril axis. Contrary to the former case, this type of fragment give an ED pattern having strong (110) and very weak (200) reflection. The weak (200) reflection suggests that such fragment is obtained from PPTA fiber by radial splitting. Figure 5(b), the ED pattern for this type of fragment, indicates that the a-axis orients almost perpendicular to the fragment surface, and that the slip plane containing hydrogen-bonded sheets lie almost parallel to the fragment surface. Under these situations, as Zaukelies' model shows, kink bands are formed perpendicular to fibril axis on the surface. In this case, despite the kink band formation, the (110) reflection always appears only on the equator.

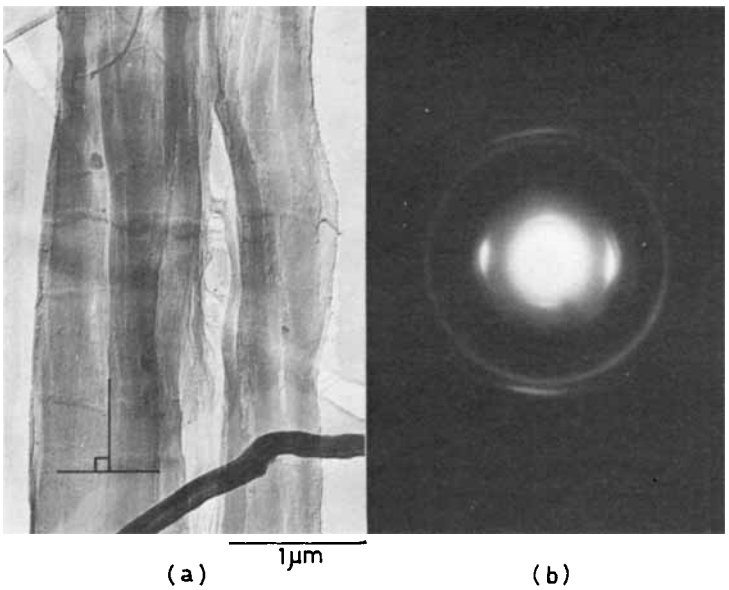

Fig. 5. Electron micrograph and corresponding electron diffraction pattern of a fibrillar fragment which was taken out from sample E by radial splitting.

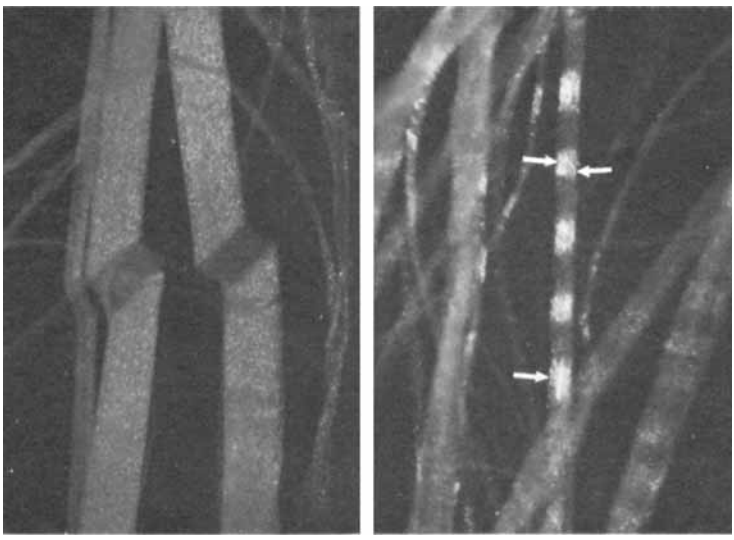

Fig. 6. [(110) + (200)] dark-field image (a) and (006) dark-field image (b) of fibrillar fragment taken out from sample E.

DF images of the unshadowed fragments were produced from ($hk0$) and ($00l$) reflections. Figure 6(a) shows an ($hk0$)-DF image of the fragment. Reflections imaged are (110) and (200). Dark bands in this DF image correspond to the kink bands such as shown in Figure 4(a). It is obvious that the dark band is attributed to the tilting of molecular chains in the kink band, because [(110) + (200)] reflections on the equator were used to produce the DF image.

On the basis of ED and DF studies of longitudinal section of PPTA fiber, Dobb et al. proposed a pleated sheet structure.[1] Simmens and Hearle[14] examined PPTA fiber by using the polarizing optical microscope at high magnification. Regular fine bands observed in the optical micrograph were identified with the pleated sheet structure.[14] Figure 6(b) shows a DF image derived from (006) reflection. The periodic organization with a spacing of about 5000 Å is observed. It can be assumed that the DF banding comes from the pleated sheet structure. Contrary to our result, Dobb did not observe the DF banding in the fibrillar fragment.[1] They supposed that the pleats collapse during sample preparation to give a flat fragment. In our case, it seems resonable to assume that the pleated sheet organization of PPTA fiber is axially compressed so as to decrease the pleat angle and, accordingly, the pleated sheet structure is retained even after the fragmentation.

White arrows in Figure 6(b) indicate a line of bright spots in a bright band of (006)-DF image. A line of spots, about 70 Å in width, may originate from an elemental fibril. It is probable that some distorted regions along the fibril axis exists in an elemental fibril.

References

1. M. G. Dobb, D. J. Johnson, and B. P. Saville, *J. Polym. Sci., Polym. Phys. Ed.*, **15**, 2201 (1977).

2. D. A. Zaukelies, *J. Appl. Phys.*, **33,** 2797 (1962).
3. K. Shigematsu, K. Imada, and M. Takayanagi, *J. Polym. Sci., Polym. Phys. Ed.*, **13,** 73 (1975).
4. N. V. Hien, S. Cooper, and J. A. Koutsky, *J. Macromol. Sci. Phys.*, **B6,** 343 (1972).
5. M. Kurokawa, T. Konishi, F. Taki, and S. Fujii, *Kobunshi-Ronbunshu*, **31,** 74 (1974).
6. M. Kurokawa and T. Ban, *J. Appl. Polym. Sci.*, **8,** 971 (1964).
7. M. Kurokawa, T. Konishi, and M. Sakano, *Sen-i Gakkaishi*, **22,** 263 (1966).
8. M. Kurokawa, T. Konishi, and M. Sakano, *Sen-i Gakkaishi*, **23,** 95 (1967).
9. M. Kurokawa, T. Konishi, and M. Sakano, *Sen-i Gakkaishi*, **24,** 101 (1968).
10. E. J. Roche, T. Takahashi, and E. L. Thomas, *Am. Chem. Soc. Symp. Ser.*, **141,** 303 (1980).
11. L. Konopasek and J. W. S. Hearle, *J. Appl. Polym. Sci.*, **21,** 2791 (1980).
12. M. G. Northholt, *Eur. Polym. J.*, **10,** 799 (1974).
13. R. Hagege, M. Jarrin, and M. Sotton, *J. Microsc.*, **115,** 65 (1979).
14. S. C. Simmens and J. W. S. Hearle, *J. Polym. Sci., Polym. Phys. Ed.*, **18,** 871 (1980).

Received February 17, 1982
Accepted August 23, 1982